Desalination and Water Treatment
www.deswater.com
doi: 10.5004/dwt.2020.25936

196 (2020) 161–176
August

Thorium(IV) removal and recovery from aqueous solutions using modified silica nanoparticles with cysteine or methionine amino acids

Latifa S. Ismail*, Fawwaz I. Khalili, Faten M. Abu Orabi

Chemistry Department, The University of Jordan, Amman 11942, Jordan, Tel. +962 6535000, emails: latifa.saeed@yahoo.com (L.S. Ismail), fkhalili@ju.edu.jo (F.I. Khalili), fatenaladwan_i@yahoo.com (F.M. Abu Orabi)

Received 12 November 2019; Accepted 3 April 2020

ABSTRACT

In this study, SiO_2 nanoparticles were modified by cysteine (SiO_2-Cys) or methionine (SiO_2-Meth) and then applied for removal thorium(IV) ion from aqueous solution. Silica nanoparticles and its modified forms were characterized by elemental analysis, scanning electron microscopy, transmission electron microscopy, X-ray diffraction, X-ray fluorescence, thermogravimetric analysis, differential scanning calorimetry, Brunauer–Emmett–Teller, zeta potential, and Fourier transform infrared analyses. Sorption of Th(IV) ion using a batch technique by silica nanoparticles, SiO_2-Cys and SiO_2-Meth was studied as a function of pH, sorbent dosage, temperature, initial concentration, and contact time. The kinetic studies show that sorption of Th(IV) ion by silica nanoparticles, SiO_2-Cys, and SiO_2-Meth was well-described by the pseudo-second-order equation. Negative values of Gibbs free energy ($\Delta G°$) suggest the spontaneity of the sorption process on silica nanoparticles and its modified forms (SiO_2-Cys) and (SiO_2-Meth). Positive values of enthalpy ($\Delta H°$) indicate the endothermic adsorption process. The sorption isotherm was better fitted by Langmuir model with maximum sorption capacity for silica nanoparticles, SiO_2-Cys and SiO_2-Meth was found to be 5.3, 8.2, and 7.0 mg/g at 25°C, respectively. Desorption studies indicate that the most favorable desorption reagent for Th(VI) is 0.1 M nitric acid.

Keywords: Modification; Silica nanoparticles; Methionine; Cysteine; Sorption; Thorium(IV)

1. Introduction

One of the serious problems that facing humanity is water pollution, contamination of water by various pollutants is an outcome of severe human activities that are increased daily. Among these pollutants are actinides, lanthanides, and other heavy metals which are of serious concern, unlike organic ones, non-biodegradable toxic substances, accumulate in the environment, and threaten human life [1]. Thorium is a naturally occurring, slightly radioactive element, and found in small amounts in most rocks, where it is about three times abundant than uranium. Thorium-232 radioactive daughter products can pose human health and ecosystems risk [2]. Therefore, removal and recovery of thorium(IV) from aqueous solution is urgent and essential. Removing thorium from aqueous solution using several techniques such as evaporation, ion exchange, solvent extraction, transport through membranes, and precipitation are generally ineffective for removal of trace amounts of pollutants and expensive [3]. Sorption has been used in industrial waste treatment for the removal of radioactive elements because of its high capacity, low cost, ease of regeneration, and no sludge produced. Different sorbents were tested for sorption of Th(IV) from aqueous solutions such as perlite [4], organoclay [5], alumina [6], activated

* Corresponding author.

carbons [7], bentonite [8], zeolite [9], and nanocomposite materials [10].

Silica, as the main part of more than 95% of all the earth's rocks and belonging to silicate compounds, it is the common name for materials composed of silicon dioxide (SiO_2). Amongst many nanoparticles being produced, silica nanoparticles have been receiving greater attention in the light of their possible uses in several scientific areas and in industrial segments such as agriculture, catalysis, energy, environment, thermal insulators and catalysts, cosmetics, medicines, printer toners, varnishes, foods, and pesticides [11]. Besides, silica nanoparticles (SiO_2-NPs) have biomedical and biotechnological applications for the controlled release of medicines and biosensors [12]. The silica surface is composed of silanol groups (Si–OH) and siloxane bridges (–Si–O–Si–). At pH higher than two, the silanol groups tend to be deprotonated as $Si–O^-$ [13]. Particles in nano-sized scale tend to agglomerate because of the high surface energy and abundant hydroxyl groups on the silica surface. So a modification to produce a hydrophobic surface is necessary to improve the dispersion and compatibility of silica nanoparticles (SiO_2-NPs) [14].

The interactions between biochemical molecules and inorganic materials have a significant impact on bionanotechnology [15], drug delivery research [16], bionanocomposite materials, and biomedical applications [17]. Therefore, numerous researches have investigated the sorption of amino acids on various materials including polymeric adsorbent [18], mineral [19], activated carbon [20], and zeolite [21]. Recently, several studies regarding the sorption of amino acids onto mesoporous silica-based adsorbents were published [22].

Cysteine and methionine are amino acids containing sulfur atom. Cysteine is a hydrophilic amino acid due to thiol group, whereas methionine is hydrophobic and has nonpolar aliphatic side chain [23]. Several biological functions embroil thiol group in cysteine [24]. Amino acids may exist either as uncharged molecule ($H_2N–CHR–COOH$) or as zwitterions ($^+H_3N–CHR–COO^-$) which depend on the pH of solution and the isoelectric point (pI) of amino acids [25]. Due to silica excellent stability and great abundance on earth, several applications have been found for the pure and the modified with amino acids or others.

The use of modified silica nanoparticles by amino acids to remove Th(IV) has not been done before. This enhance the uptake of Th(IV) due to the large surface area of nanosilica and the functional groups of the attached amino acids in comparison to the values in literature (see Table 6).

The aim of this study is to modify silica nanoparticles 10–20 nm with cysteine or methionine amino acids as adsorbents for removal of Th(IV) ions from aqueous solutions. Sorption of Th(IV) by unmodified and modified silica nanoparticles with cysteine or methionine, at different time, pH, temperature, and metal ions concentration at constant ionic strength have been studied using batch technique. To understand and explain the sorption behavior, the Langmuir, Freundlich, and Dubinin–Radushkevich (D–R) models have been used to model the obtained data. The kinetic and thermodynamic parameters of sorption have been calculated. Also, desorption process after sorption was studied.

2. Experimental

2.1. Chemicals

All reagents used in this study were of analytical grade reagents. Silicon dioxide nanopowder, 10–20 nm particle size (Brunauer–Emmett–Teller (BET)), 99.5% trace metals basis, L-methionine reagent grade ≥ 98% (high performance liquid chromatography) and L-cysteine 98% cell culture tested from Sigma Aldrich. Hydrochloric acid (HCl) 37%, nitric acid (HNO_3) 69%, and glacial acetic acid from Tedia, sodium hydroxide pellets (NaOH) from SDS vorte partenaire chimie, sodium perchlorate ($NaClO_4$) from Acros, cadmium chloride monohydrat ($CdCl_2·H_2O$) from Merck (USA), ninhydrin from Riedel de Haen, thorium(IV) nitrate tetrahydrate ($Th(NO_3)_4·4H_2O$) from BDH Chemicals Ltd., Poole, England. Arsenazo(III) indicator from Janseen chimica while absolute ethanol (99.5%) and acetone from SOLVOCHEM (Netherlands).

2.2. Instruments

Weighing was done using RADWAG® AS 220 R2 (Poland), electronic balance. Filtration was done using 0.4 μm nylon syringe filters. The pH of solution was measured using EUTECH pH-meter. Fourier-transform infrared spectroscopy (FTIR) spectra were done using Thermo Nicolet NEXUS 670 (USA) FTIR spectrophotometer with KBr disc. Centrifugation was done using (DJB Lab Care-AIC PK 130) at 2,500 rpm speed. Elemental analyses were obtained with a Euro EA3000 CHNS-O elemental analyzer (Milan, Italy). Thermal gravimetric analysis (TGA) were carried using NETZCH STA (simultaneous thermal analyzer) 409 PG/PC (Germany) thermal analyzer in the temperature range (0°C–800°C) at a heating rate of 20°C/min. Thermal stability and melting was carried by NETZCH (Germany) differential scanning calorimeter (DSC) 204 F1 in the temperature range (0°C–800°C) at a heating rate of 10°C/min. X-ray diffraction (XRD) was measured using Philips X pert PW 3060 (Netherlands), operated at 45 kV and 40 mA. The chemical composition of the samples was determined by X-ray fluorescence (Shimadzu XRF-1800, Japan). The shape with three dimensional (3D) and surface morphology was examined with Nanoscale Characterization and Fabrication Laboratory (NCFL's) Field Electron and Ion Company (FEI) QUANTA 600 Field Emission Gun (FEG) scanning electron microscope (SEM). Samples were shaken using GFL-85 thermostatic shaker. The concentration of the Th(IV) ion was determined using Vis-spectrophotometer from METASH model V-5100, and a 1.0 cm quartz cell. BET, 1938 method was used to measure specific surface area (SSA) of the powder from sorption desorption of N_2 at 77.3 K with Nova 220e surface area and pore size analyzer. Zeta potential was carried using Microtrac Zetatrac.

2.3. Modification of silica nanoparticles with cysteine or methionine

A 60.0 g of the silica nanoparticles was mixed with 60.0 g ± 0.1 mg of cysteine in 1 L deionized water for 48 h. On the other hand, a 60.0 g of the silica nanoparticles was mixed with 24.0 g ± 0.1 mg of methionine in 1 L deionized

water for 48 h. Then the mixture in both cases SiO_2-Meth or SiO_2-Cyst was filtered using centrifugation and the solid was dried in vacuum oven at 25°C to a constant weight. The amount of cysteine or methionine remaining in the filtrate solution was determined by vis-spectrophotometer using Cd-ninhydrine solution after constructing up an analytical calibration curve [26].

2.4. Sorption experiments

Kinetic studies were used to determine the equilibrium time for sorption of Th(IV) by silica nanoparticles (SiO_2-NPs) and its modified forms using batch technique. Shaking 0.1g ± 0.1 mg of the silica nanoparticles and its modified forms in 100 mL plastic bottle with 25.0 mL of 50 mg/L Th(IV) ion solution at pH 3.0, the contact time varied from 15 to 1,440 min at 25°C, 35°C, and 45°C. The mixture was filtered with 0.45 μm nylon micro filter and the amount of Th(IV) ions remaining in the filtrate was determined by vis-spectrophotometer using arsenazo(III) indicator [27].

The percent uptake (%) of Th(IV) ions from aqueous solution and the sorption capacity (q_e) have been calculated using the following equations:

$$\text{Uptake}(\%) = \frac{(C_0 - C_e)}{C_0} \times 100\% \quad (1)$$

$$q_e = \frac{(C_0 - C_e)V}{m} \quad (2)$$

where C_0 is the initial Th(IV) concentration (mg/L), C_e the remaining concentration of Th(IV) in solution at equilibrium, V (L) the volume of Th(IV) solution, and m (g) the mass of the silica nanoparticles (SiO_2-NPs) or its modified forms.

2.5. Modeling of sorption isotherms and kinetics

In order to understand the adsorption mechanism of Th(IV) onto silica nanoparticles and its modified forms, kinetic investigations were carried using the following models:

Pseudo-first-order:

$$\ln(q_e - q_t) = \ln q_e - k_1 t \quad (3)$$

and pseudo-second-order:

$$\frac{t}{q_t} = \frac{1}{k_2 q_e^2} + \frac{t}{q_e} \quad (4)$$

where q_e and q_t (mg/g) are the amount of Th(IV) adsorbed onto silica nanoparticles (SiO_2-NPs) and its modified forms at equilibrium and time t (min) respectively. k_1 (1/min) is the rate constant for the pseudo-first-order and k_2 is the rate constant for the pseudo second-order (g/mg min) adsorption process [28].

Three types of isotherm models were used to study the sorption of Th(IV) onto silica nanoparticles and its modified forms: Langmuir [29], Freundlich [30], and Dubinin–Radushkevich [31]. The sorption isotherms of Th(IV) onto silica nanoparticles and its modified forms were carried out by shaking 0.1 g silica nanoparticles or its modified forms with 25.0 mL of metal ion solution of different concentrations ranging from 10 to 50 mg/L at pH 3 for 1 h and at different temperatures (25°C, 35°C, and 45°C).

The following formulas are used to study the adsorption isotherms:

- Langmuir equation (Form I):

$$\frac{C_e}{q_e} = \frac{1}{(q_m K_L)} + \left(\frac{1}{q_m}\right) C_e \quad (5)$$

- Freundlich equation:

$$\text{Log} q_e = \log K_F + \frac{1}{n} \log C_e \quad (6)$$

- Dubinin–Radushkevich equations:

$$\ln q_e = \ln q_{max} - \beta\varepsilon^2 \quad (7)$$

The Polanyi potential ε, equals to:

$$\varepsilon = RT \ln\left(1 + \frac{1}{C_e}\right) \quad (8)$$

2.6. Desorption experiments

The desorption of Th(IV) ion was carried using batch technique. By loading 0.5 ± 0.0001 g silica nanoparticles or its modified forms; (SiO_2-Cys) and (SiO_2-Meth) with 25.0 mL of 50 ppm of Th(IV) solution in 50.0 mL centrifuge tube and shaking for 24 h, then centrifuged, decanted. The remaining solid was washed with deionized water several times. In the same centrifuge tube, desorption was tested using 25.0 mL of two eluting agents, 1.0 M HNO_3 and 0.1 M HNO_3 on two different samples of silica nanoparticles and its modified forms (SiO_2-Cys) and (SiO_2-Meth) to recover adsorbed metal ions. Desorption procedure was repeated three times to completely remove metal ions. The concentration of metal ions in the collected three elutes was determined by vis-spectrophotometer at 660 nm wavelength to calculate percentage removal of Th(IV) ion.

3. Results and discussion

3.1. Characterization of silica nanoparticles and its modified forms

The silica nanoparticles and its modified forms; (SiO_2-Cys) and (SiO_2-Meth) were characterized by elemental analysis, FTIR, XRF, XRD, SEM, transmission electron microscope (TEM), N_2-sorption/desorption isotherm (BET), zeta potential (ζ), TGA, and differential scanning calorimetry (DSC).

3.1.1. Elemental analysis

Increasing the percentage of carbon, hydrogen, and nitrogen in modified silica nanoparticles comparing with unmodified forms indicated a successful surface functionalization of silica nanoparticles with cysteine or methionine

and this result agrees with the following FTIR, XRD, and XRF results (Table 1).

3.1.2. Fourier-transform infrared spectroscopy

The FTIR spectra of silica nanoparticles (SiO_2-NPs) and its modified forms SiO_2-Cys and SiO_2-Meth are shown in Fig. 1. The FTIR analysis was performed in order to establish the changes in the functional groups of the silica nanoparticles and its modified form to insure the modification. Fig. 1 shows characteristic peaks for silica nanoparticles at 1,065; 800; and 598 cm^{-1} which were related to the asymmetric, symmetric, and bending modes of Si–O–Si, respectively and 949.75 cm^{-1} for Si–OH stretching vibration of the silanol group [32]. Also; Fig. 1 showed additional peaks appearing for modified silica nanoparticles with cysteine and methionine at 2,983 (2,968 cm^{-1} for methionine), 1,743; 1,369 cm^{-1}, which were related to N–H stretching, C=O stretching and COO^- symmetric stretching [33,35]. The differences in the spectra for silica nanoparticles and modified silica nanoparticles with cysteine or methionine indicated that amino acids were successfully attached to silanol group or silica surface.

Table 1
Elemental analysis results for silica nanoparticles and its modified forms

Sample	%C	%H	%N
SiO_2-NPs	1.9	1.6	–
SiO_2-Cys	12.8	2.6	4.2
SiO_2-Meth	4.4	1.7	0.7

3.1.3. X-ray diffraction

Fig. 2 represents the XRD pattern for silica nanoparticles and its modified forms; (SiO_2-Cys) and (SiO_2-Meth). It showed a broad peak at 2θ = 22.50°, which is a known characteristic peak for amorphous silica [36], and two sharp peaks at 2θ = 18.95° and 33.16° for (SiO_2-Cys) related to monoclinic crystalline cysteine [37]. While, the modified silica nanoparticles with methionine (SiO_2-Meth) pattern showed two sharp peaks at 2θ = 5.16° and 23.21° related to monoclinic crystalline methionine [38]. The presence of sharp peaks in XRD pattern of the modified silica nanoparticles is a proof of modification of crystalline amino acids.

3.1.4. X-ray fluorescence

XRF was used to determine the elemental composition of the silica nanoparticles and its modified forms; (SiO_2-Cys) and (SiO_2-Meth). The results presented in Table 2 showed the high content of sulfur in the modified silica nanoparticles with cysteine or methionine which indicated the association of cysteine or methionine with silica nanoparticles.

3.1.5. Zeta potential

Table 3 shows that ζ potential values of unmodified silica nanoparticles and its modified forms values in water at pH 3.0 are negative, which indicates negative surface charge. The large negative value of unmodified silica nanoparticles (–69.2 mV) indicated a highly stable dispersed silica nanoparticles [39]. However, the ζ potential of modified silica nanoparticles with cysteine (–69.7 mV) and with methionine (–71.9 mV) are more negative than

Fig. 1. FTIR spectra for the silica nanoparticles and its modified forms.

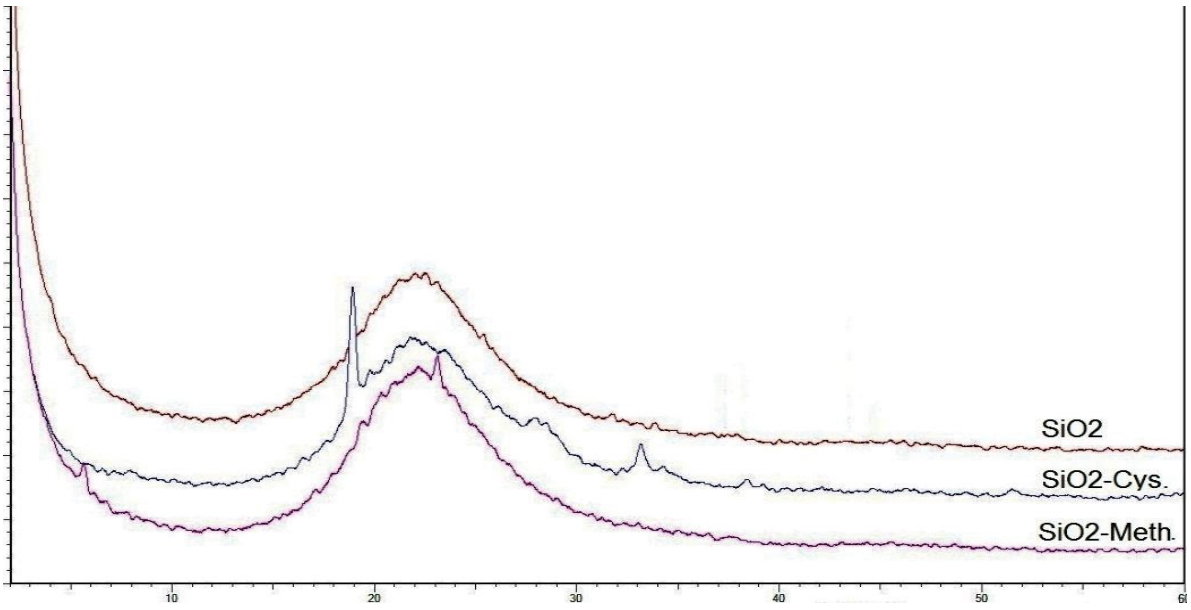

Fig. 2. X-ray diffraction pattern of silica nanoparticles and its modified forms.

Table 2
Chemical composition (% weight) of silica nanoparticles and its modified forms

Chemical composition	SiO_2-NPs (% weight)	SiO_2-Cys (% weight)	SiO_2-Meth (% weight)
Si	98.8%	82.0%	86.8%
S	1.2%	17.9%	13.1%

the unmodified form. This proves the presence of amino acids in zwitterion forms and that ammonium groups interact with silanol groups while the carboxylate groups are free [40,41] and a successful surface functionalization of silica nanoparticles (SiO_2-NPs) with cysteine or methionine amino acids.

3.1.6. Scanning electron microscopy

The morphology for silica nanoparticles (SiO_2-NPs) and its modified forms were investigated using SEM. All SEM images (Fig. 3) indicated that the particles having irregular morphology and agglomerate with various sizes in the modified forms due to the presence of cysteine or methionine resulting in particles size more than 1 μm [42].

3.1.7. Transmission electron microscope

TEM was used to investigate the morphology (particle size and shape) of silica nanoparticles (SiO_2-NPs) and its modified forms; (SiO_2-Cys) and (SiO_2-Meth). Fig. 4 clearly showed the spherical like morphology of silica nanoparticles and its modified forms. Figs. 4a–c showed particle size about 23 nm for silica nanoparticles, 16 nm for SiO_2-Cys and 14 nm for SiO_2-Meth with average particle size of 10–20 nm [43]. This decrease in particle size is due to sample preparation with sonication. This result agrees with zeta potential results; the high value of negative charge on the surface of modified silica nanoparticles with cysteine or methionine increases the repulsion between particles which lead to decrease in the agglomeration of particles and particle size [39].

Table 3
Main characteristics of silica nanoparticles and its modified forms

Sample	ζ (mV)	S_{BET} (m^2/g)	Average pore diameter (nm)
SiO_2-NPs	–69.2	139.9	10.0
SiO_2-Cys	–69.7	92.0	7.7
SiO_2-Meth	–71.9	121.5	7.6

3.1.8. Nitrogen sorption/desorption isotherm (BET)

Brunauer–Emmett–Teller (BET) equation has been used to calculate the SSA (m^2/g) and the average pore diameter (nm) for silica nanoparticles (SiO_2-NPs) and its modified forms; (SiO_2-Cys) and (SiO_2-Meth). Table 4 shows the nitrogen sorption/desorption isotherms results. The silica nanoparticles (SiO_2-NPs) exhibited type IV sorption isotherm with a H1 hysteresis type as shown in Fig. 5 [44]. The modified silica nanoparticles with cysteine (SiO_2-Cys) have the lowest SSA (92.0 m^2/g) than the one modified with

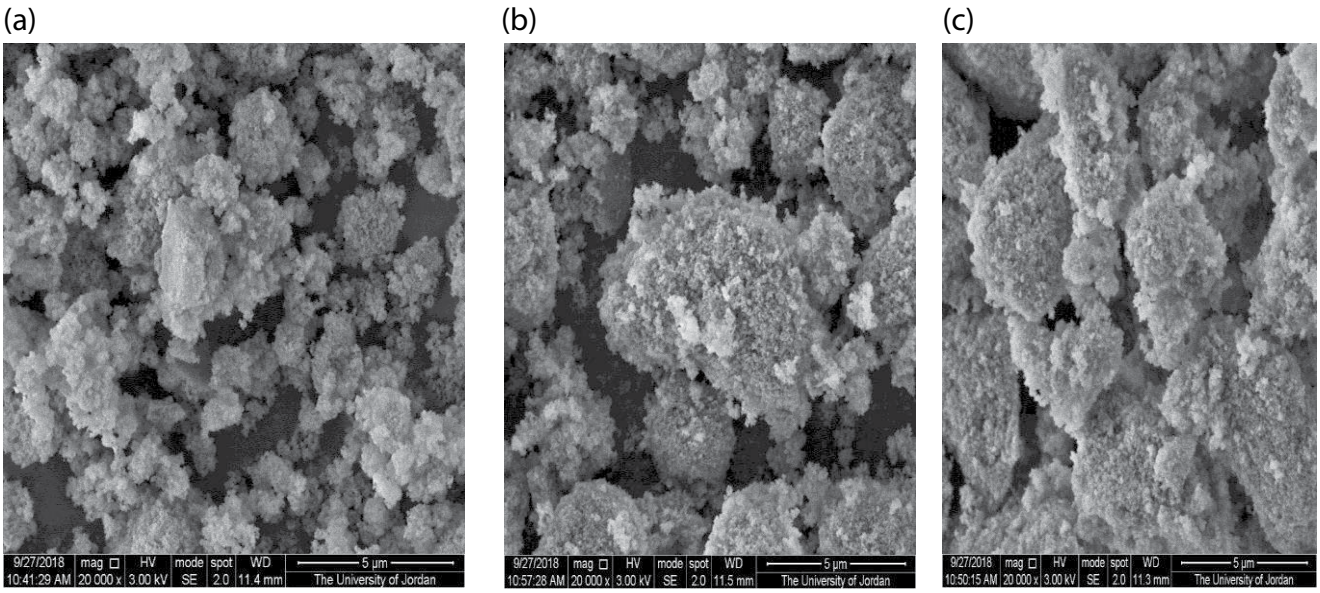

Fig. 3. SEM micrographs of (a) silica nanoparticles, (b) SiO_2-Cys, and (c) SiO_2-Meth.

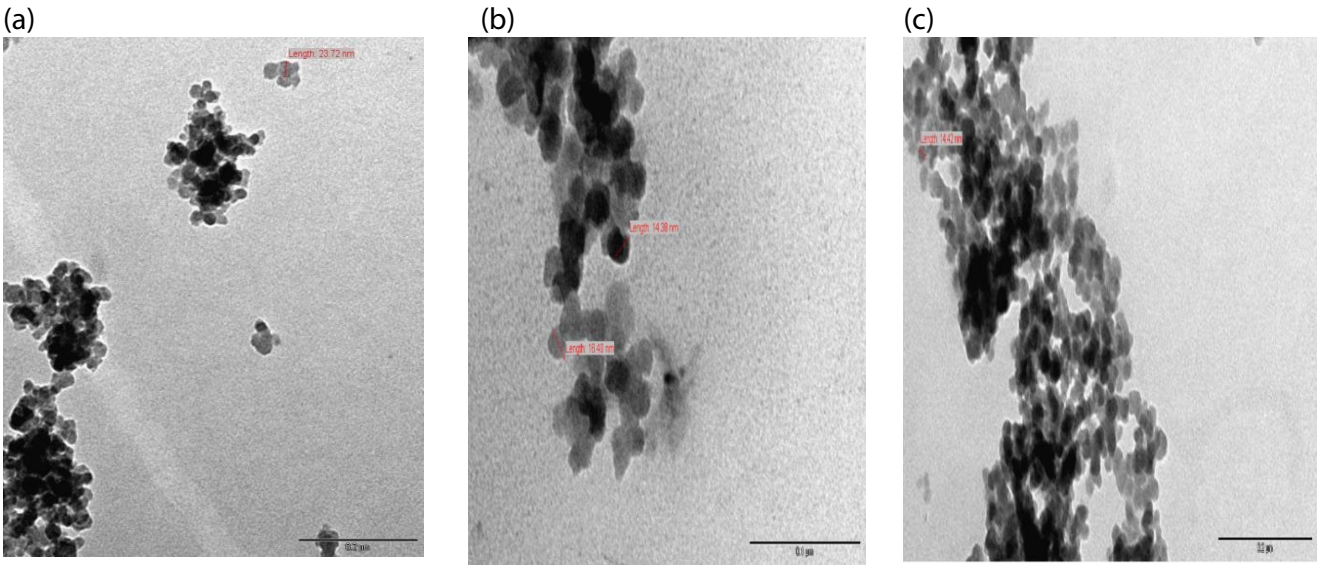

Fig. 4. TEM micrograph of (a) silica nanoparticles, (b) SiO_2-Cys, and (c) SiO_2-Meth.

Table 4
Kinetic parameters for sorption of thorium(IV) by silica nanoparticles and its modified forms at 25°C

Pseudo-second-order model parameters	SiO_2	SiO_2-Cys	SiO_2-Meth
k_2 (g/mg min)	0.041	0.061	0.050
q_e (mg/g) calculated	5.050	8.260	7.090
q_e (mg/g) experimental	5.030	8.210	7.060
R^2	1.000	1.000	1.000

methionine (121.5 m^2/g) and silica nanoparticles (139.9 m^2/g). This ensures the modification and agrees with elemental analysis and the percentage loading of cysteine on silica nanoparticles surface, which is more than that of methionine [45]. The average pore diameter for silica nanoparticles is 10.0 nm, which classified it as mesoporous silica [44], whereas the average pore diameter for SiO_2-Cys and SiO_2-Meth is 7.7 and 7.6 nm, respectively. The small decrease in average pore diameter with the addition of cysteine or methionine results from the occupation of pore space by the amino acids.

3.1.9. Thermal properties

3.1.9.1. Thermogravimetric analysis

Fig. 6 shows the TGA thermogram of silica nanoparticles (SiO_2-Nps) and its modified forms with cysteine or methionine. The TGA thermogram for silica nanoparticles (Fig. 6) showed a weight loss (about 6%wt.) after 100°C, which is related to the elimination of physically adsorbed water on the surface [46]. The TGA thermogram for modified silica nanoparticles with methionine (Fig. 6) showed two weight loss stages. The first weight loss stage before 200°C, can be related to the physically adsorbed water and the second small weight loss (about 13%wt.) at 300°C attributed to the decomposition of methionine [47]. Also, the TGA thermogram showed two weight loss stages for modified silica with cysteine (Fig. 6). The first stage occurred before 200°C, which is similar to that of SiO_2-Meth, whereas the second stage (about 26%wt.) at 230°C due to the decomposition of cysteine [48]. The percentage weight loss of SiO_2-Cys is more than that of SiO_2-Meth, which is due to the higher percentage loading of cysteine than methionine by silica nanoparticles.

3.1.9.2. Differential scanning calorimetry

DSC method has been used to evaluate the degree of purity of a compound [38]. Fig. 7 shows glass transition temperature at 90°C for silica nanoparticles and its modified forms; (SiO_2-Cys) and (SiO_2-Meth), as a result of the presence of the amorphous silica nanoparticles. Whereas Fig. 7 shows the DSC thermogram analysis for modified silica nanoparticles with cysteine (SiO_2-Cys). The presence of melting transition temperature at 230°C as broad peak indicated that cysteine is not pure and it is associated with silica nanoparticles surface [48]. Also, Fig. 7 shows the DSC thermogram analysis for SiO_2-Meth and the melting transition temperature showed as a weak peak at 205°C due to the low percentage loading of methionine on surface of silica nanoparticles and this agrees with thermogravimetric analysis results.

3.2. Effect of adsorbent dose

The removal efficiency of Th(IV) increases with increasing silica nanoparticles (SiO_2-NPs) mass and reaches 98.0% uptake at 0.5 g (Fig. 8), which is a consequence of more binding sites available for Th(IV) ions sorption [49]. Also Fig. 8 shows sorption capacity (q_e) for Th(IV) ions, it was noticed that 0.1 g of silica nanoparticles has greatest sorption

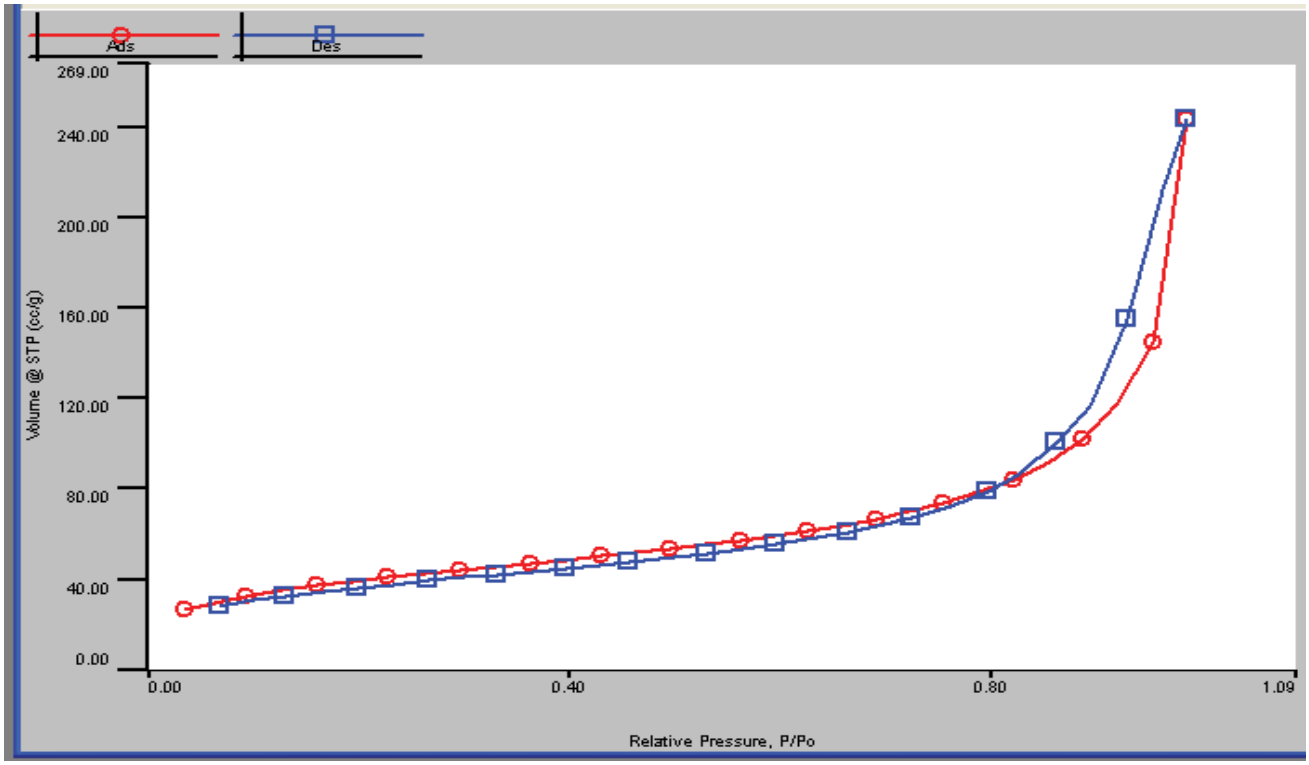

Fig. 5. Nitrogen sorption/desorption isotherm for silica nanoparticles.

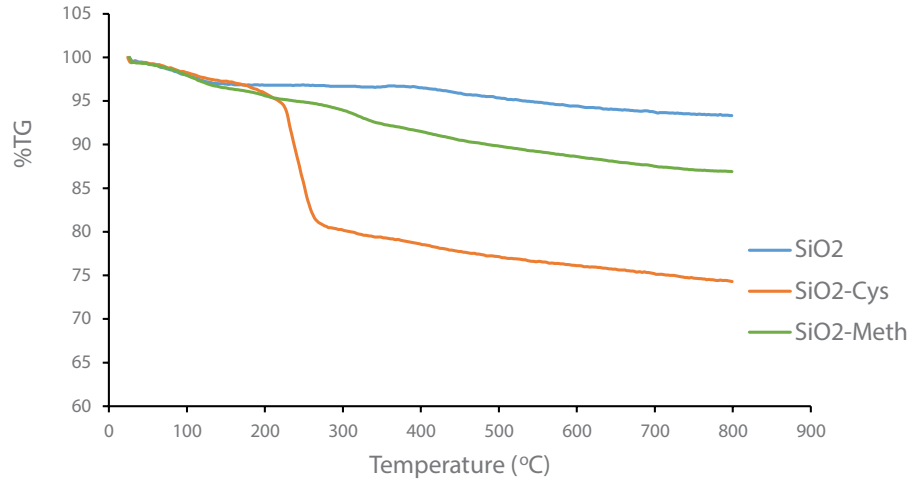

Fig. 6. TGA thermogram of silica nanoparticles and its modified forms.

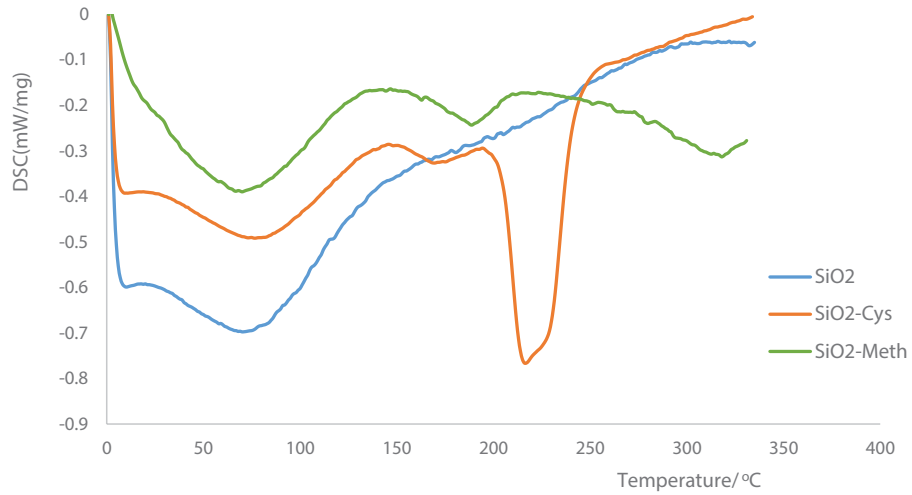

Fig. 7. DSC thermograms of silica nanoparticles and its modified forms.

capacity. Due to economic, environmental and experimental obligations, 0.1 g of adsorbent is used throughout the following experiments.

3.3. Effect of pH

The pH of the aqueous solution plays an important role and influences the metal speciation and surface metal-binding sites [50]. Adsorption was studied by varying the pH from 1 to 4 for fixed Th(IV) concentration onto silica nanoparticles (SiO_2-NPs) and its modified forms, which increased with increasing pH (Fig. 9a). Increasing the negative surface charge density of silica nanoparticles and its modified forms with increasing pH can be a result of the ionization of surface silanol groups [51]. In this study, it was supposed that there is an electrostatic interaction between the positively charged Th(IV) hydrolysis products and the negative charged group of silica nanoparticles and its modified forms. The adsorption of Th(IV) by silica nanoparticles and its modified forms were done at pH 3.0 because of the hydrolysis of Th(IV) ions above pH 3.0.

3.4. Effect of temperature

Experiments were performed at 25°C, 35°C, and 45°C to determine the effect of temperature on sorption of Th(IV) by silica nanoparticles (SiO_2-NPs) and its modified forms. Fig. 9b shows increasing percentage uptake of Th(IV) ions with temperature from 25°C to 45°C indicating that the sorption mechanism for Th(IV) ions was energy dependent and endothermic [52].

3.5. Effect of initial concentration

The sorption of Th(IV) ions onto silica nanoparticles (SiO_2-NPs) and its modified forms were carried out by varying the initial Th(IV) concentration from 10 to 50 mg/L (Fig. 9c). At low initial solution concentration of Th(IV), the surface area and the availability of adsorption sites were relatively high, and the Th(IV) ions were easily adsorbed and removed. At higher initial concentration, the total available adsorption sites are limited, thus resulting in a decrease in percentage removal of Th(IV) ions.

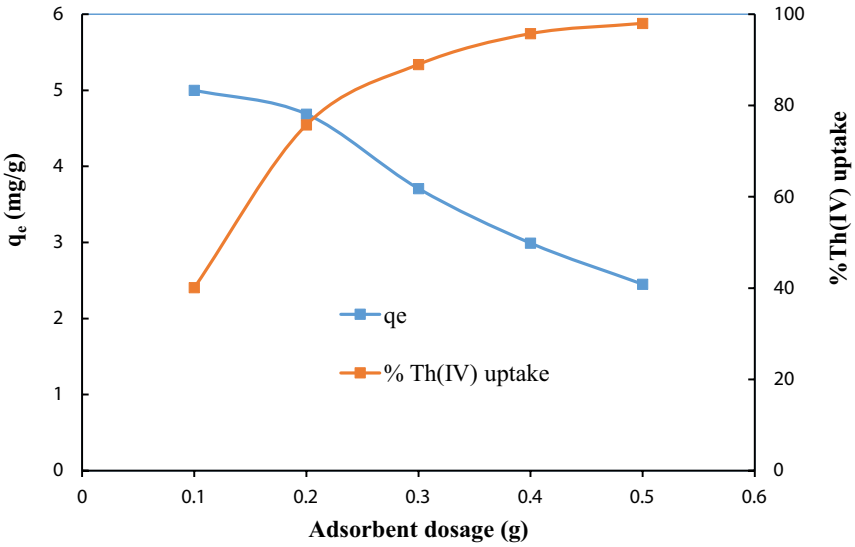

Fig. 8. Effect of adsorbent dosage on the sorption of Th(IV) onto silica nanoparticles (initial concentration 50 ppm and 25°C).

3.6. Effect of contact time and sorption kinetic models

From the results shown in Fig. 10, it is clear that the percentage uptake of thorium(IV) by (SiO_2-Cys) is higher than that for (SiO_2-Meth) and for unmodified silica nanoparticles (SiO_2-Nps) and relatively fast. These results can be explained by the binding of cysteine to metal ions (presence of carboxylate group and –SH group) and percentage loading of cysteine on silica nanoparticles.

The linear plots of (t/q_t vs. time) were displayed in Fig. 11 for thorium(IV) adsorbed on silica nanoparticles and its modified forms; (SiO_2-Cys) and (SiO_2-Meth). Table 4 shows the values of R^2 = 1.00 for pseudo-second-order model and the calculated sorption capacity q_e was closer to the experimental sorption capacity q_e, indicating that the pseudo-second-order kinetic model is highly suitable to describe the three sorption process of thorium(IV) by silica nanoparticles and its modified forms. This propose that chemisorption is the rate-controlling step for sorption of thorium(IV) by silica nanoparticles and its modified forms [3].

3.7. Effect of initial concentrations and sorption isotherm models

As shown in Fig. 12, the sorption capacities (q_e) of thorium(IV) increased with increasing initial concentration of thorium(IV) at pH 3. The reason is that increasing initial concentration of thorium(IV) ions provide a significant driving force to overcome the mass transfer resistance between solid phase and aqueous phase, which enhanced the sorption process [53].

The calculated isotherm parameters are shown in Table 5. As shown in Figs. 13 and 14, the sorption of thorium(IV) ion onto unmodified and modified forms of silica nanoparticles shows high correlation coefficients ($R^2 > 0.9$) for both the Langmuir and Freundlich isotherm models.

The possible reason is that both the monolayer and multilayer sorption existed in the sorption process of thorium(IV) and the presence of homogenous and heterogeneous sites on the surface, these results agreed with SEM images.

The values of K_L (Table 5) for sorption of thorium(IV) by (SiO_2-Meth) were more than the other two adsorbents, indicating that sorption bonding energy onto (SiO_2-Meth) was more than the other two [54].

It was found that the obtained R_L (separation factor) values were greater than 0 but less than 1 as shown in Table 5, indicating that the sorption processes of thorium(IV) ions onto silica nanoparticles and its modified forms were favorable. In addition, the values of R_L approach zero (the completely ideal irreversible case) rather than unity (which represents a completely reversible case).

The Freundlich isotherm is the second mathematical model used to describe the sorption of metal ions present in solution on heterogeneous surfaces. The Freundlich constant K_F (mg g^{-1}) and n are characteristic constants related to the relative sorption capacity of the sorbent and the intensity of sorption, respectively. Table 5 shows that the Freundlich constant (K_F) for the sorption of thorium(IV) onto silica nanoparticles and its modified forms increased with increasing temperature, due to the endothermic nature [55]. The K_F value of the Freundlich equation also indicates that (SiO_2-Meth) has a very high sorption capacity for thorium(IV) ions than silica nanoparticles and (SiO_2-Cys). The values of n, represent the degree of favorability of sorption (Tables 5), were greater than one, indicating that the sorption of thorium(IV) onto silica nanoparticles and its modified forms was favorable [56]. Based on the values of n, the sorption of thorium(IV) ions by SiO_2-Meth is more favorable than by silica nanoparticles and (SiO_2-Cys).

The D–R isotherm model is more general than Langmuir isotherm as it rejects the homogenous surface or constant sorption potential. As illustrated in Table 5, the magnitude of free energy of sorption (E) can give a good idea about the overall mechanism of the sorption process. Since the values of E are less than 8.00 (kJ/mol) indicates that physical forces affect the sorption [57].

Essentially, silica nanoparticles and its modified forms show good sorption performance for Th(IV) at pH 3 than

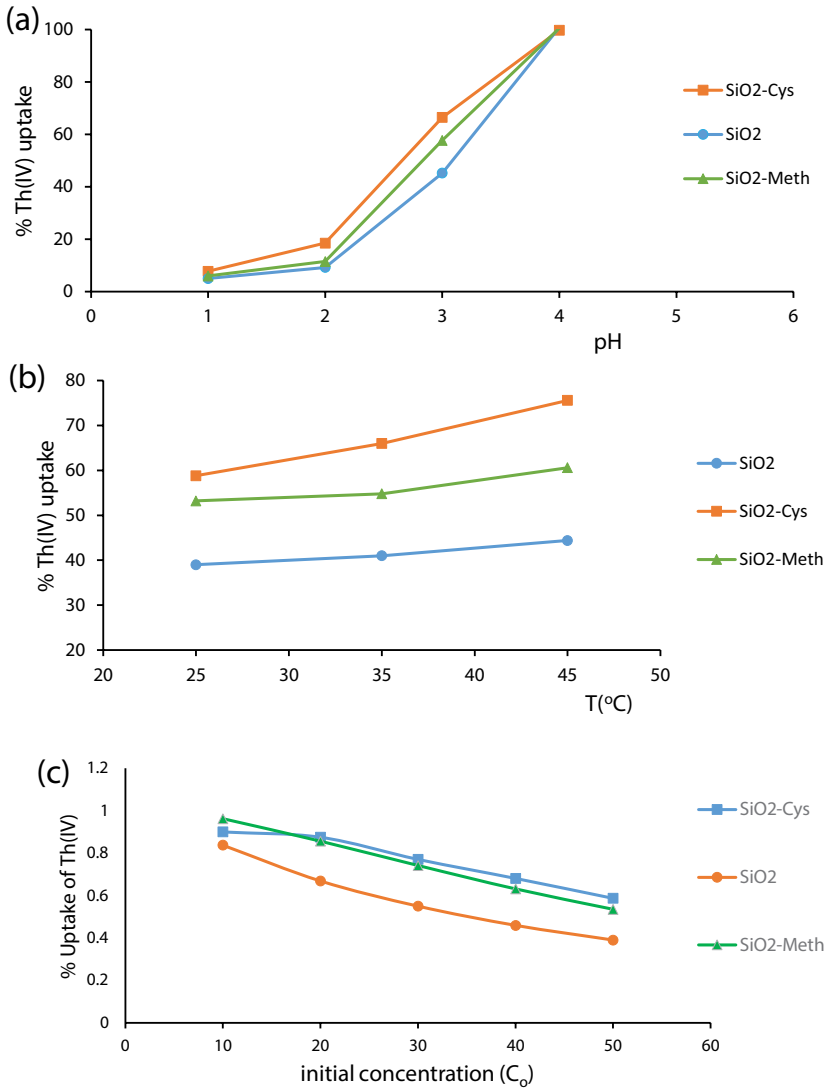

Fig. 9. Percentage uptake of Th(IV) by 0.1 g of silica nanoparticles and its modified forms; (a) Vs pH at 25°C and 24 h, (b) Vs temperatures at pH 3 and 24 h, and (c) Vs initial concentration (C_0) at pH 3, 25°C, and 1 h.

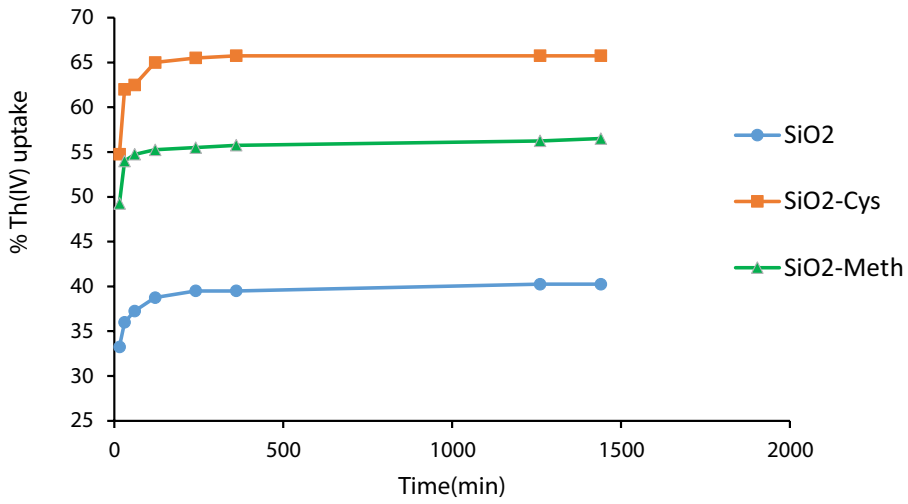

Fig. 10. Thorium(IV) percentage uptake vs. time by silica nanoparticles and its modified forms (SiO_2-Cys) (SiO_2-Meth) at pH 3.0 and 25°C.

Table 5
Langmuir, Freundlich, and Dubinin–Radushkevich isotherm parameters for sorption of thorium(IV) by silica nanoparticles and its modified forms at different temperatures

T (°C)	Langmuir isotherm				Freundlich isotherm			Dubinin–Radushkevich (D–R)			
	R^2	q_m (mg/g)	K_L (L/mg)	R_L	R^2	n (L/mg)	K_F (mg/g)	R^2	β (mol²/kJ²)	q_m (mg/g)	E (kJ/mol)
Silica nanoparticles											
25.0	0.996	5.347	0.294	0.063	0.991	3.413	1.860	0.857	0.526	4.320	0.975
35.0	0.997	5.494	0.440	0.043	0.990	3.984	2.300	0.868	0.277	4.560	1.480
45.0	0.997	5.780	0.793	0.024	0.989	4.926	2.960	0.866	0.062	4.970	2.840
SiO_2-Cys											
25.0	0.999	8.260	0.387	0.049	0.926	2.66	2.600	0.950	0.378	6.520	1.150
35.0	0.998	8.853	0.649	0.029	0.939	2.570	3.600	0.909	0.107	7.390	2.160
45.0	0.998	10.305	0.970	0.020	0.957	2.301	4.430	0.892	0.067	7.860	2.730
SiO_2-Meth											
25.0	0.996	7.042	0.676	0.0287	0.990	3.952	3.170	0.864	0.036	2.130	3.720
35.0	0.999	7.142	1.217	0.016	0.963	4.219	3.620	0.895	0.055	6.090	3.010
45.0	0.998	7.874	1.245	0.015	0.986	4.366	4.100	0.960	0.029	7.150	4.150

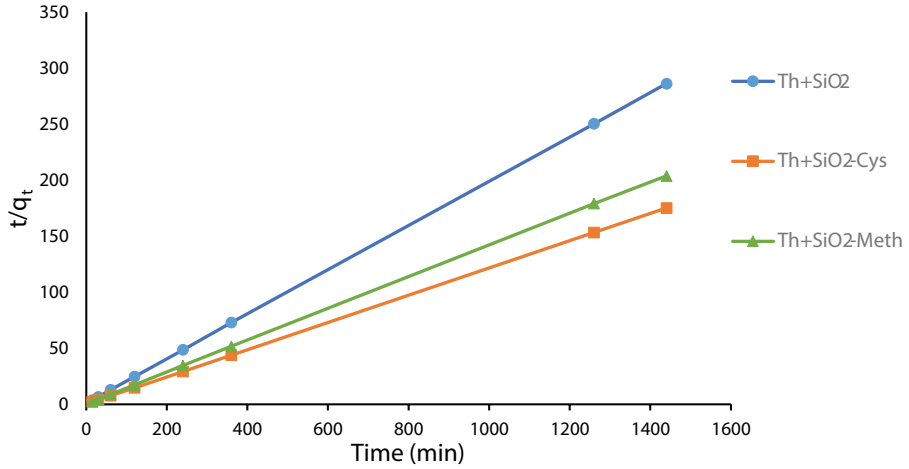

Fig. 11. Pseudo-second-order sorption kinetics of thorium(IV) by silica nanoparticles and its modified forms (SiO_2-Cys) and (SiO_2-Meth) at pH 3.0 and 25°C.

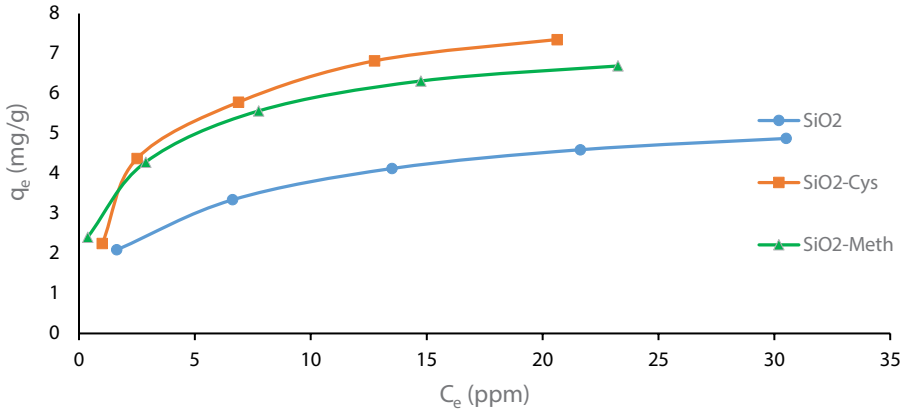

Fig. 12. Plots of adsorption isotherms of thorium(IV) with silica nanoparticles or its modified forms, at pH 3 and at 25°C.

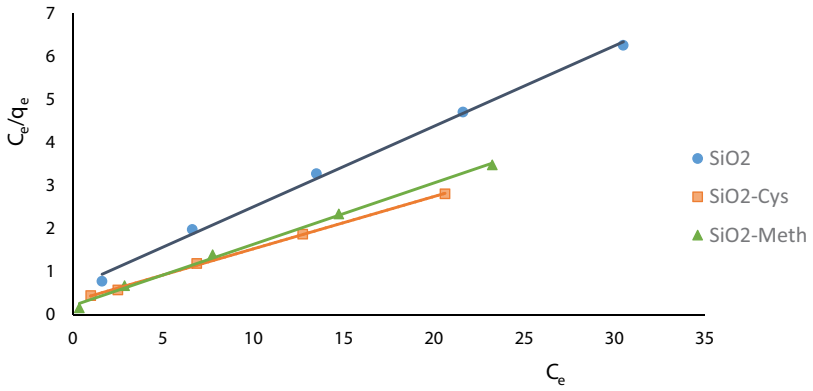

Fig. 13. Langmuir adsorption isotherms of thorium(IV) ion onto silica nanoparticles or its modified forms, at pH 3 and 25°.

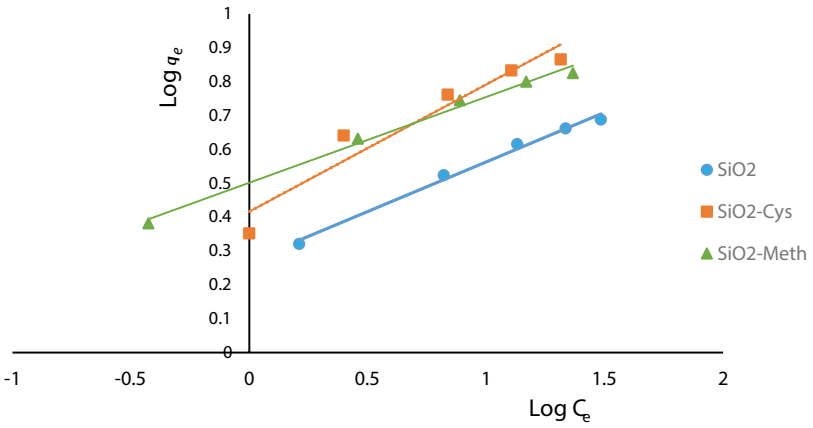

Fig. 14. Freundlich adsorption isotherms of thorium(IV) ion onto silica nanoparticles or its modified forms, at pH 3 and 25°C.

other adsorbents which were reported in literature and listed in Table 6.

3.8. Thermodynamic studies

Thermodynamic functions can be determined using the distribution coefficient $K_d = q_e/C_e$ which depends on temperature. The change in free energy ($\Delta G°$), enthalpy ($\Delta H°$), and entropy ($\Delta S°$) associated with the adsorption process were calculated by using the following equations:

$$\Delta G° = \Delta H° - T\Delta S° \quad (9)$$

where R is the universal gas constant (8.314 J/mol K) and T is temperature (K).

$$\ln K_d = \frac{\Delta S°}{R} - \frac{\Delta H°}{RT} \quad (10)$$

According to the Eq. (10), $\Delta H°$ and $\Delta S°$ functions can be obtained from the slope and intercept of the plot of $\ln K_d$ vs. $1/T$, respectively as shown in Table 7 and Fig. 15.

Table 7 show that (SiO_2-Meth) has the highest value of $\Delta G°$, which indicated that sorption of thorium(IV) onto (SiO_2-Meth) is more energetically favorable than silica nanoparticles and (SiO_2-Cys) and this agreed with K_d values [62]. The positive values of $\Delta H°$ (Table 7) indicated that the sorption of thorium(IV) on silica nanoparticles and its modified forms is endothermic. Also, if the value of $\Delta H°$ is lower than 40 kJ/mol, the sorption can be recognized as a physical process as explained from the value of free energy of sorption (E) in (D–R) isotherm model. Physical sorption is caused mainly by van der Waals and electrostatic forces between adsorbate molecules and atoms which compose the adsorbent surface. One possible explanation of the positive values of enthalpy $\Delta H°$ is that the metal ions are well-solvated and in order for the metal ions to be adsorbed, they have to lose part of their hydration sphere. This dehydration process of the ions requires energy and this energy of dehydration supersedes the exothermicity of the ions getting attached to the surface [55]. The positive values of $\Delta S°$ for silica nanoparticles and its modified forms (Table 7) indicate the increase in randomness at the solid/solution interface during the sorption process and the affinity of adsorbent for metal ions used. The adsorbed water molecules, which are displaced by the adsorbate species, gain more translational energy than that lost by the thorium(IV) ions, thus allowing the prevalence of randomness in the system. Also, the dehydration of metal ions increases the randomness of the system [63].

Table 6
Comparison between adsorption capacity of Th(IV) on various adsorbents

Adsorbents	pH	Adsorption capacity (mg/g)	References
Gibbsite	4.0	4.00	[58]
Bentonite	4.0	2.75	[59]
Perlite	4.5	5.00	[4]
Silica	3.5	1.00	[60]
Silica modified with humic acid	3.5	2.05	[60]
Silica modified with Fulvic acid	3.5	2.45	[60]
Humic acid-silica gel composite	2.5	5.60	[61]
Silica nanoparticles	3.0	5.30	This work
Silica nanoparticles modified with cysteine (SiO_2-Cys)	3.0	8.20	
Silica nanoparticles modified with methionine (SiO_2-Meth)	3.0	7.00	

Table 7
Thermodynamic parameters for sorption of thorium(IV) by silica nanoparticles and its modified forms at 25°C

Adsorbent	$\Delta G°$ (kJ/mol)	$\Delta H°$ (kJ/mol)	$\Delta S°$(J/mol K)
SiO_2-NPs	–1.41	33.85	118.32
SiO_2-Cys	–1.51	21.30	76.53
SiO_2-Meth	–3.10	11.43	48.78

3.9. Desorption studies

Desorption is important from two points of view: first, the recovery of radionuclide and subsequent use in nuclear energy cycle, secondly the regeneration of sorbent for reuse in other sorption processes. Fig. 16 and Table 8 show the values of percentage cumulative recovery of thorium(IV) form loaded silica nanoparticles and its modified forms using two concentrations of nitric acid. It was found that desorption of thorium(IV) using 0.1 M HNO_3 is more efficient than 1.0 M HNO_3 [64], also more desorption percentage for thorium(IV) with 48.1% achieved from silica nanoparticles than modified forms. The lowest value of cumulative recovery percentage for (SiO_2-Meth) than silica nanoparticles and (SiO_2-Cys) explain its greatest tendency in holding thorium(IV) ions. Modified silica nanoparticles with methionine (SiO_2-Meth) could be used in removal of thorium(IV) ions from solution and concentrating them to be removed as solid radioactive wastes.

4. Conclusions

In the present work, modification of silica nanoparticles with cysteine or methionine amino acids; (SiO_2-Cys) and (SiO_2-Meth) have been done and characterized by FTIR, SEM, TEM, XRD, XRF, TGA, DSC, zeta potential, nitrogen sorption/desorption isotherm and elemental analysis. Removal of thorium(IV) by silica nanoparticles and its modified forms from aqueous solutions using batch sorption experiments have been carried out under different experimental conditions. Desorption of loaded thorium(IV) ion onto silica nanoparticles and its modified forms were investigated at 25°C using 0.1 and 1.0 M nitric acid. Modified silica nanoparticles with cysteine (SiO_2-Cys) showed a relatively higher percentage uptake for thorium(IV) ions than silica nanoparticles and modified silica nanoparticles with methionine. Thorium(IV) sorption onto silica nanoparticles and its modified forms are highly dependent on pH, and the adsorbed metal ions increased with increasing pH. Kinetic studies indicate that

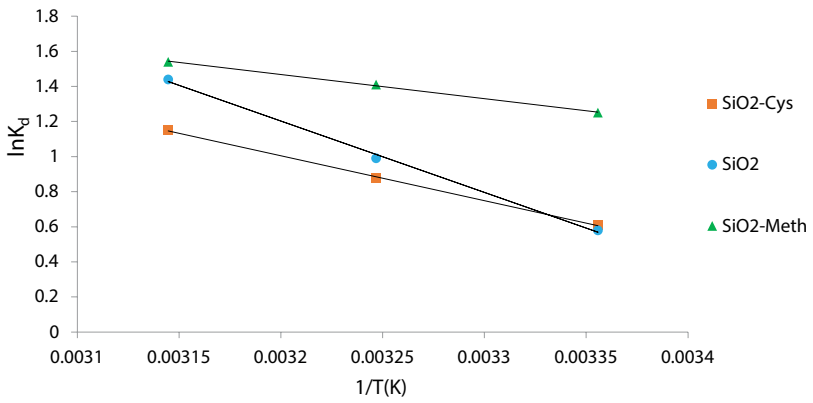

Fig. 15. Plots of lnK_d vs. 1/T for thorium(IV) on silica nanoparticles and its modified forms.

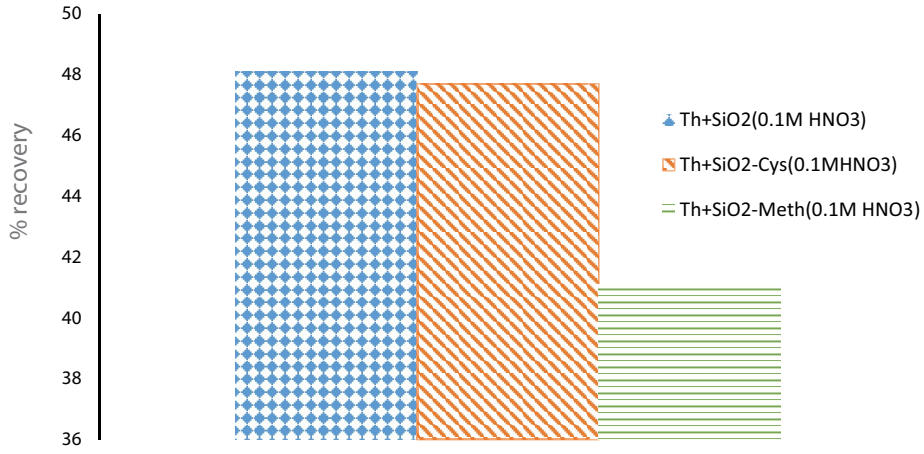

Fig. 16. Percentage recovery of thorium(IV) form silica nanoparticles and its modified forms.

Table 8
Desorption percentage of thorium(IV) loaded onto silica nanoparticles and its modified forms

	SiO_2-NPs		SiO_2-Cys		SiO_2-Meth	
Recovery stage	0.1 M HNO_3	1.0 M HNO_3	0.1 M HNO_3	1.0 M HNO_3	0.1 M HNO_3	1.0 M HNO_3
1st 10.0 mL	25.3%	25.0%	28.6%	23.6%	30.8%	26.5%
2nd 10.0 mL	19.0%	16.0%	16.8%	14.8%	8.3%	7.0%
3rd 10.0 mL	3.8%	2.0%	2.3%	2.3%	2.0%	1.9%
%Cumulative recovery	48.1%	43.0%	47.7%	40.7%	41.1%	35.4%

sorption needs one hour to reach equilibrium, and its data fitted well with the pseudo-second-order model. Langmuir sorption isotherm showed better fitting than Freundlich and Dubinin–Radushkevich sorption isotherm models with maximum sorption capacity (q_m) for thorium(IV) by (SiO_2-Cys) of 10.3 at 45°C. Thermodynamic parameters showed that the sorption process is endothermic and spontaneous. The best percent recovery of thorium(IV) loaded onto silica nanoparticles and its modified forms obtained using 0.1 M HNO_3 after three recovery stages and the highest percent recovery for thorium(IV) was achieved from silica nanoparticles than the modified forms.

References

[1] B. Volesky, Detoxification of metal-bearing effluents: biosorption for the next century, Hydrometallurgy, 59 (2001) 203–216.
[2] V. Hollriegl, M. Greiter, A. Giussani, U. Gerstmann, B. Michalke, P. Roth, U. Oeh, Observation of changes in urinary excretion of thorium in humans following ingestion of a therapeutic soil, J. Environ. Radioact., 95 (2007) 149–160.
[3] H. Dolatyari, M. Yaftian, S. Rostamnia, Removal of uranium(VI) ions from aqueous solutions using Schiff base functionalized SBA-15 mesoporous silica materials, J. Environ. Manage., 169 (2016) 8–17.
[4] Z. Talip, M. Eral, U. Hicsonmez, Sorption of thorium from aqueous solutions by perlite, J. Environ. Radioact., 100 (2009) 139–143.
[5] S. Simsek, D. Baybas, M.C. Koçyigit, H. Yıldırım, Organoclay modified with lignin as a new adsorbent for removal of Pb^{2+} and UO_2^{2+}, J. Radioanal. Nucl. Chem., 299 (2014) 283–292.
[6] Z. Guo, X. Yu, F. Guo, Z. Tao, Th(IV) sorption on alumina: effects of contact time, pH, ionic strength and phosphate, J. Colloid Interface Sci., 288 (2014) 14–20.
[7] C. Kutahyali, M. Eral, Selective sorption of uranium from aqueous solutions using activated carbon prepared from charcoal by chemical activation, Sep. Purif. Technol., 40 (2004) 109–114.
[8] F. Khalili, N. Salameh, M. Shaybe, Sorption of uranium(VI) and thorium(IV) by Jordanian bentonite, J. Chem., 2013 (2012) 1–14.
[9] F. Khalili, M. Al-Shaybe, Sorption of thorium(IV) and uranium(VI) by Tulul al-Shabba Zeolitic Tuff, Jordan, Jordan J. Earth Environ. Sci., 2 (2009) 108–119.
[10] A.A. Alqadami, M. Naushad, Z.A. Alothman, A.A. Ghfar, Novel metal–organic framework (MOF) based composite material for the sequestration of U(VI) and Th(IV) metal ions from aqueous environment, ACS Appl. Mater. Interfaces, 9 (2017) 36026–36037.
[11] T.K. Barik, B. Sahu, V. Swain, Silica nanoparticles-from medicine to pest control, Parasitol. Res., 103 (2008) 253–258.
[12] R. Subbiah, M. Veerapandian, K.S. Yun, Nanoparticles: functionalization and multifunctional applications in biomedical sciences, Curr. Med. Chem., 17 (2010) 4559–4577.
[13] C. Mathe, S. Devineau, J. Aude, G. Lagniel, C. Chedin, V. Legros, M. Mathon, Structural determinants for protein sorption/nonsorption to silica surface, PLoS One 8 (2013) 81346.
[14] N.S. Nam, D.N. Khang, L.Q. Tuan, L.T. Son, Surface modification of silica nanoparticles by hexamethyldisilazane and n-butanol, Int. J. Environ. Technol. Sci., 2 (2016) 31–37.
[15] C.E. Ashley, E.C. Carnes, G.K. Phillips, D. Padilla, P.N. Durfee, P.A. Brown, T.N. Hanna, J. Liu, B. Phillips, M.B. Carter, The targeted delivery of multicomponent cargos to cancer cells by nanoporous particle-supported lipid bilayers, Nat. Mater.,10 (2011) 389–397.

[16] D. Tarn, C.E. Ashley, M. Xue, E.C. Carnes, J.I. Zink, C.J. Brinker, Mesoporous silica nanoparticle nanocarriers: biofunctionality and biocompatibility, Acc. Chem. Res., 46 (2013) 792–801.
[17] S.V. Patwardhan, F.S. Emami, R.J. Berry, S.E. Jones, R.R. Naik, O. Deschaume, H. Heinz, C.C. Perry, Chemistry of aqueous silica nanoparticle surfaces and the mechanism of selective peptide sorption, J. Am. Chem. Soc., 134 (2012) 6244–6256.
[18] D.S. Grzegorczyk, G. Carta, Sorption of amino acids on porous polymeric adsorbents—II. Intraparticle mass transfer, Chem. Eng. Sci., 51 (1996) 819–826.
[19] J. Ikahsan, B.B. Johnson, J.D. Wells, M.J. Angove, Sorption of aspartic acid on kaolinite, J. Colloid Interface Sci., 273 (2004) 1–5.
[20] A. Vinu, K.Z. Hossain, G.S. Kumar, K. Ariga, Adsorption of L-histidine over mesoporous carbon molecular sieves, Carbon, 44 (2006) 530–536.
[21] J.E. Krohn, M. Tsapatsis, Amino acid sorption on zeolite beta, Langmuir, 21 (2005) 8743–8750.
[22] H. Faghihian, M. Nejati-Yazdinejad, Equilibrium study of sorption of L-cysteine by natural bentonite, Clay Miner., 44 (2009) 125–133.
[23] D.M. Townsend, K.D. Tew, H. Tapiero, Sulfur containing amino acids and human disease, Biomed. Pharmacother., 58 (2004) 47–55.
[24] M.L. Conte, U. Jakob, D. Reichmann, Oxidative Stress and Redox Regulation, Springer, USA, 2013.
[25] J.F. Lambert, Sorption and polymerization of amino acids on mineral surfaces: a review, Origins Life Evol. Biosphere, 38 (2008) 211–242.
[26] E. Doi, D. Shibata, T. Matoba, Modified calorimetric ninhydrin methods for peptidase assay, Anal. Biochem., 118 (1981) 173–184.
[27] A.H. Orabi, Determination of uranium after separation using solvent extraction from slightly nitric acid solution and spectrophotometric detection, J. Radiat. Res. Appl. Sci. 6 (2013) 1–10.
[28] S. Azizian, Kinetic models of sorption: a theoretical analysis, J. Colloid Interface Sci., 276 (2004) 47–52.
[29] I. Langmuir, The sorption of gases on plane surfaces of glass, mica and platinum, J. Am. Chem. Soc., 40 (1918) 1361–1403.
[30] H. Freundlich, Over the sorption in solution, J. Phys. Chem., 57 (1906) 385–470.
[31] M.M. Dubinin, L.V. Radushkevich, Equation of the characteristic curve of activated charcoal, Chem. Zentralbl., 1 (1947) 875–890.
[32] F. Fan, D. Pan, H. Wu, H. Zhang, W. Wu, Succinamic acid grafted nano silica for the preconcentration of U(VI) from aqueous solution, Ind. Eng. Chem. Res., 56 (2017) 2221–2228.
[33] A. Khataee, A. Movafeghi, F. Nazari, F. Vafaei, M. Dadpour, Y. Hanifehpour, S. Joo, The toxic effects of L-cysteine-capped cadmium sulfide nanoparticles on the aquatic plant *Spirodela polyrrhiza*, J. Nanopart. Res., 16 (2014) 2774–2784.
[34] S.F. Parker, Assignment of the vibrational spectrum of L-cysteine, Chem. Phys., 424 (2013) 75–79.
[35] M. Wolpert, P. Hellwig, Infrared spectra and molar absorption coefficients of the 20 alpha amino acids in aqueous solutions in the spectral range from 1800 to 500 cm^{-1}, Spectrochim. Acta, Part A, 64 (2006) 987–1001.
[36] V. Jafari, A. Allahverdi, Synthesis and characterization of colloidal silica nanoparticles via an ultrasound assisted route based on alkali leaching of silica fume, Int. J. Nanosci. Nanotechnol., 10 (2014) 145–152.
[37] H. Chen, H. Bian, J. Li, X. Guo, X. Wen, J. Zheng, Molecular conformations of crystalline L-cysteine determined with vibrational cross angle measurements, J. Phys. Chem. B, 117 (2013) 15614–15624.
[38] J. Hautala, S. Airaksinen, N. Naukkarinen, O. Vainio, A. Juppo, Evaluation of new flavors for feline mini-tablet formulations, J. Excipients Food Chem., 5 (2014) 80–100.
[39] I. Dakova, P. Vasileva, I. Karadjova, Cysteine modified silica submicrospheres as a new sorbent for preconcentration of Cd(II) and Pb(II), Bulg. Chem. Commun., 43 (2011) 210–216.
[40] K. Kim, H. Kim, W. Lee, C. Lee, T. Kim, J. Lee, J. Jeong, S. Paek, J. Oh, Surface treatment of silica nanoparticles for stable and charge-controlled colloidal silica, Int. J. Nanomed., 9 (2014) 29–40.
[41] M. Du, Y. Zheng, Modification of silica nanoparticles and their application in UDMA dental polymeric composites, Polym. Compos., 28 (2007) 198–207.
[42] S. Sompech, T. Dasri, S. Thaomola, Preparation and characterization of amorphous silica and calcium oxide from agricultural wastes, Orient. J.Chem., 32 (2016) 1923–1928.
[43] A. Fuad, N. Mufti, M. Diantoro, K.S. Septa, Synthesis and characterization of highly purified silica nanoparticles from pyrophyllite ores, AIP Conf. Proc., 1719 (2016) 30020–30025.
[44] K. Sing, D.H. Everett, R.A.W. Haul, L. Moscou, R.A. Pierotti, J. Rouquerol, T. Siemieniewska, Reporting physisorption data for gas/solid systems with special reference to the determination of surface area and porosity, Pure Appl. Chem., 57 (1985) 603–619.
[45] M. Chaves, K. Valsaraj, R. DeLaune, R. Gambrell, P. Buchler, Mercury uptake by biogenic silica modified with L-cysteine, Environ. Technol., 32 (2011) 1615–1625.
[46] J. Wu, G. Ma, P. Li, L. Ling, B. Wang, Surface modification of silica nanoparticles with acrylsilane-containing tertiary amine structure and their effect on the properties of UV-curable coating, J. Coat. Technol. Res., 11 (2014) 387–395.
[47] N. Belachew, D. Rama Devi, K. Basavaiah, Facile green synthesis of L-methionine capped magnetite nanoparticles for adsorption of pollutant Rhodamine B, J. Mol. Liq., 224 (2016) 713–720.
[48] I.M. Weiss, C. Muth, R. Drumm, H. Kirchner, Thermal decomposition of the amino acids glycine, cysteine, aspartic acid, asparagine, glutamic acid, glutamine, arginine and histidine, BMC Biophys., 11 (2018) 1–15.
[49] T. Fan, Y. Liu, B. Feng, G. Zeng, C. Yang, M. Zhou, H. Zhou, X. Wang, Biosorption of cadmium(II), zinc(II) and lead(II) by *Penicillium simplicissimum*: isotherms, kinetics and thermodynamics, J. Hazard. Mater., 160 (2008) 655–661.
[50] M.W. Clark, J.J. Harrison, T.E. Payne, The pH-dependence and reversibility of uranium and thorium binding on a modified bauxite refinery residue using isotopic exchange techniques, J. Colloid Interface Sci., 356 (2011) 699–705.
[51] F. Khalili, A. Khalifa, G. Al-Banna, Removal of uranium(VI) and thorium(IV) by insolubilized humic acid originated from Azraq soil in Jordan, J, Radioanal. Nucl. Chem., 311 (2017) 1375–1392.
[52] Y. Huang, Y. Hu, L. Chen, T. Yang, H. Huang, R. Shi, P. Lu, C. Zhong, Selective biosorption of thorium(IV) from aqueous solutions by ginkgo leaf, PLoS One, 13 (2018) 193659.
[53] Z. Naseem, H. Bhatti, S. Sadaf, S. Noreen, S. Ilyas, Sorption of uranium(VI) by *Trapa bispinosa* from aqueous solution, effect of pretreatments and modeling studies, Desal. Water Treat., 57 (2016) 11121–11132.
[54] M. Ebrahimi-Gatkash, H.N. Younesi, A. Heidari, Amino-functionalized mesoporous MCM-41 silica as an efficient adsorbent for water treatment: batch and fixed-bed column sorption of the nitrate anion, Appl. Water Sci.,7 (2015) 1887–1901.
[55] U.H. Kaynar, M. Ayvacıklı, U. Hiçsönmez, S.C. Kaynar, Removal of thorium(IV) ions from aqueous solution by a novel nanoporous ZnO: isotherms, kinetic and thermodynamic studies, J. Environ. Radioact., 150 (2015) 145–151.
[56] S. Chegrouche, A. Mellah, M. Barkat, A. Aknoun, Kinetics and isotherms for uranium(VI) sorption from aqueous solutions by goethite, Am. J. Mater. Sci., 3 (2016) 6–12.
[57] R. Donat, A. Akdogan, E. Erdem, H. Cetisli, Thermodynamics of Pb^{2+} and Ni^{2+} sorption onto natural bentonite from aqueous solutions, J. Colloid Interface Sci., 286 (2005) 43–52.
[58] Z. Hongxia, D. Zheng, T. Zuyi, Sorption of thorium(IV) ions on gibbsite: effects of contact time, pH, ionic strength, concentration, phosphate and fulvic acid, Colloids Surf., A, 278 (2006) 46–52.
[59] D.L. Zhao, S.J. Feng, C.L. Chen, S.H. Chen, D. Xu, X.K. Wang, Adsorption of thorium(IV) on MX-80 bentonite: effect of pH, ionic strength and temperature, Appl. Clay Sci., 41 (2008) 17–23.
[60] C. Chen, X. Wang, Sorption of Th(IV) to silica as a function of pH, humic/fulvic acid, ionic strength, electrolyte type, Appl. Radiat. Isot., 65 (2007) 155–163.

[61] E. Prasetyo, K. Toyoda, Sol–gel synthesis of a humic acid-silica gel composite material as low-cost adsorbent for thorium and uranium removal, J. Radioanal. Nucl. Chem., 310 (2016) 69–80.
[62] L. Xia, K. Tan, X. Wang, W. Zheng, W. Liu, C. Deng, Uranium removal from aqueous solution by banyanleaves: equilibrium, thermodynamic, kinetic and mechanism studies, J. Environ. Eng., 139 (2013) 887–895.
[63] F. Khalili, G. Al-Banna, Sorption of uranium(VI) and thorium(IV) by insolubilized humic acid from Ajloun soil – Jordan, J. Environ. Radioact., 146 (2015) 16–26.
[64] C. Liu, X. Liang, J. Liu, W. Yuan, Desorption of copper ions from the polyamine functionalized adsorbents: behaviors and mechanisms, Adsorpt. Sci. Technol., 34 (2016) 455–468.